Light-Controlled Ion Switching: Direct Observation of the Complete Nanosecond Release and Microsecond Recapture Cycle of an Azacrown-Substituted $[(bpy)Re(CO)_3L]^+$ Complex

Jared D. Lewis, Robin N. Perutz, and John N. Moore*

Department of Chemistry, The University of York, Heslington, York, YO10 5DD, United Kingdom

Received: July 12, 2004

A $[(bpy)Re(CO)_3L]^+$ complex (bpy = 2,2′-bipyridine) in which L contains an azacrown ether (MacQueen, D. B.; Schanze, K. S. *J. Am. Chem. Soc.* **1991**, *113*, 6108) acts as a reversible light-controlled switch of alkali and alkaline earth metal cations bound to the azacrown, as observed directly by time-resolved UV−vis spectroscopy. Excitation to the metal-to-ligand charge-transfer (MLCT) state of the metal-complexed form, $[(bpy)Re(CO)_3L]^+$-M^{n+}, results in cation release on the nanosecond time scale for $M^{n+} = Li^+$, Na^+, Ca^{2+}, and Ba^{2+}, with Li^+ and Na^+ being released more rapidly than Ca^{2+} and Ba^{2+}; by contrast, Mg^{2+} is not released. After decay to the ground state, $[(bpy)Re(CO)_3L]^+$ recaptures metal cations on the microsecond time scale to restore the starting thermal equilibrium. A multistep rebinding mechanism is observed for Li^+ and Na^+, in which the cation attaches initially to the azacrown nitrogen atom before binding to the equilibrium position within the azacrown ring. The excited states and other intermediates in the cation release-and-recapture cycle have been observed directly in real time, and their decay rate constants have been determined as a function of cation identity, enabling a generalized light-controlled cation-switching mechanism to be developed for this generic molecular design.

Introduction

The increasing demand to control chemical, optical, electrical, and mechanical processes or signals on the nanometer scale has stimulated the development and study of molecular switches that can be converted from one state to another by an external stimulus.[1−3] Switches that are capable of the controlled release or capture of guest species have potential applications in triggering chemical or biochemical reactions, or for transporting species across membranes, and one important goal is the development of reversible switches that can undergo repeated release-and-recapture cycles. Molecular switching is typically effected by chemical, optical, or electrical stimuli, and light is the preferred stimulus in many cases because its delivery can be controlled precisely in space and in time.

Light-controlled molecular switches can provide a jump in the concentration of metal cations in solution.[4−29] Caged compounds, in which a photoinduced covalent bond-breaking reaction gives an irreversible concentration jump, have been developed as very effective systems to study the action of metal cations such as Ca^{2+} on biological systems.[4−10] Switches in which a photoisomerization reaction changes the binding constant, either increasing or decreasing the concentration of free metal cations, have also been developed:[11−21] this mechanism gives bistable switching, in principle, although the process may not be fully reversible if switching occurs between two photostationary-state mixtures. The possibility of cation switching that is induced directly by the electronic changes resulting from photoexcitation has also been explored,[22−29] using molecular designs drawn from the wide range of chromo- and fluoroionophores developed as cation sensors,[30−34] and direct observations of the reversible switching of Sr^{2+} and Ba^{2+} have recently been reported.[26,27]

The development of reversible light-controlled ion switches is aided by progress in the design and characterization of molecular sensors that combine a receptor, a linking unit, and a chromophore.[30−37] Many of these sensors use a change in fluorescence intensity to report on cation binding, based on photoinduced electron transfer quenching that is either promoted or inhibited by cation binding. Azacrown ethers generally provide responsive sensors because they act as receptors for metal cations, and direct electronic communication with the chromophore is facilitated by conjugation via the azacrown nitrogen atom. This design offers good prospects for light-controlled cation ejection if the chromophore has a charge-transfer excited state that produces a partial positive charge on the azacrown nitrogen atom, thereby lowering the cation binding constant.[22−29] However, a fast back electron-transfer reaction may limit its effectiveness by returning the molecule to its ground state at a rate that competes with cation release into bulk solvent, thus resulting in rapid relaxation to the initial equilibrium with the cation remaining bound within the azacrown.[22−25]

Many of the chromophoric cation sensors and switches reported to date are organic molecules.[30−34] Among organometallic examples,[38−51] several incorporate the $(N−N)Re(CO)_3L$ group (N−N = α-diimine ligand)[46−51] and have used a change in the intensity of the emission from the $d\pi(Re) \rightarrow \pi^*(N−N)$ metal-to-ligand charge-transfer (MLCT) excited state to report on cation binding. MacQueen and Schanze reported one early example, a $[(bpy)Re(CO)_3L]^+$ complex (ReAZBAP$^+$; Scheme 1),[46] which they demonstrated to act as a sensor via an increase in the luminescence intensity on binding Na^+, Ca^{2+}, or Ba^{2+} cations. They reported the MLCT state emission lifetime and quantum yield and proposed a mechanism in which rapid intramolecular electron transfer in the MLCT state creates a ligand-to-ligand charge-transfer (LLCT) state in which charge separation is effected between the bpy and azacrown ligands

* Corresponding author. E-mail: jnm2@york.ac.uk.

10.1021/jp0469214 CCC: $27.50
Published on Web 09/18/2004

SCHEME 1: Structures of ReAZBAP$^+$ and ReBAP$^+$

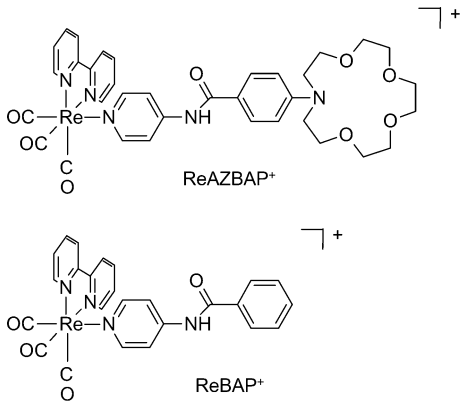

(Scheme 2); the emission yield increases on binding because the electrostatic effect of the metal cation on the azacrown nitrogen atom makes electron transfer thermodynamically unfavorable and prolongs the lifetime of the MLCT state. Most interestingly, they found that the MLCT emission lifetime and quantum yield of the ReAZBAP$^+$-M^{n+} complexes depend on the identity of the metal cation, and they proposed a novel mechanism in which cations are ejected from the azacrown in the MLCT state. MacQueen and Schanze noted that the effect of cation ejection limits the applicability of ReAZBAP$^+$ as a cation sensor,[46] but their studies have prompted us to explore its potential as a light-controlled cation switch because of its generic design: it contains an azacrown receptor linked to a chromophore with a charge-transfer excited state in which electron-density is transferred away from the azacrown, and it contains a transition-metal redox center that may mediate the electron transfer reactions whose rates are likely to control the overall photochemistry. Moreover, this design is one in which ion switching should be fully reversible because the proposed mechanisms are based on changes only in electronic state: relaxation to the ground state should result in metal cation recapture as the starting equilibrium is reestablished.

In a recent communication,[27] we demonstrated the reversible photoinduced switching of Ba^{2+} by a novel derivative of ReAZBAP$^+$ in which the linking amide group is replaced by an alkyne group; our studies demonstrated the effect for this metal cation, but they did not reveal the underlying mechanisms. In this paper, we report detailed studies of the photochemical mechanisms of ReAZBAP$^+$ in the presence of several metal cations. In a preparatory study of ReAZBAP$^+$ in the absence of cations,[52] we used time-resolved UV−vis absorption (TRVIS) and emission spectroscopy to substantiate the validity of Scheme 2 and to determine the TRVIS spectra of the MLCT and LLCT states. The forward and back electron-transfer reactions were observed to occur on the pico- and nanosecond time scales, respectively, and their rate constants were rationalized in terms

SCHEME 2: Photochemical Mechanism for ReAZBAP$^+$

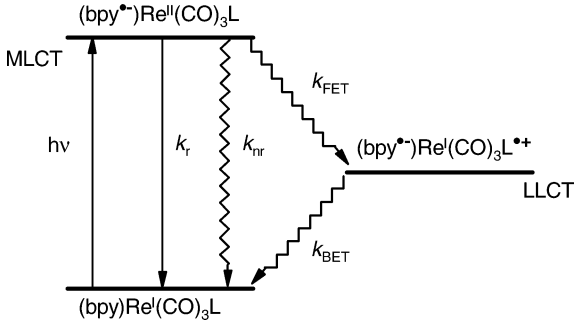

of electron-transfer theory. Parallel studies showed that excited-state electron transfer does not occur for ReBAP$^+$ (Scheme 1), in which the azacrown is absent, nor in ReAZBAP$^+$-H$^+$, in which the azacrown nitrogen atom is protonated. Here, we report time-resolved UV−vis absorption and emission studies of ReAZBAP$^+$-M^{n+} complexes in which Li^+, Na^+, K^+, Mg^{2+}, Ca^{2+}, or Ba^{2+} are bound to the azacrown. These studies demonstrate that ReAZBAP$^+$ acts as a reversible light-controlled ion switch of Li^+, Na^+, Ca^{2+}, and Ba^{2+} by direct observations of their complete release-and-recapture ion-switching cycles in real time: excited-state cation release occurs on the nanosecond time scale, with the resultant cation-free ground-state ReAZBAP$^+$ complex then recapturing the cations on the microsecond time scale. Importantly, our studies enable us to develop a general light-controlled ion-switching mechanism for this generic molecular design: the cycle is based solely on changes in electronic state, and the dependence of the release and recapture rates on the identity of the metal cation are quantified.

Experimental Procedures

The rhenium complexes (Scheme 1) and (bpy)Re(CO)$_3$Cl were prepared according to literature methods.[46,52,53] Samples were prepared in spectroscopic or HPLC grade acetonitrile (Aldrich), except for ReAZBAP$^+$-M^{n+}, where anhydrous acetontirile (Aldrich) was used as received and handled under nitrogen. HCl, $LiClO_4$, $NaClO_4$, $KClO_4$, K(NCS), $Mg(ClO_4)_2$, $Ba(ClO_4)_2$, and $Ca(ClO_4)_2$ (Aldrich) were used as received, except that the barium and calcium salts were dried under vacuum at 230 °C overnight prior to use. Perchlorate salts were used in all cases except potassium, where KNCS was used because of the low solubility of $KClO_4$ in acetonitrile. ReAZBAP$^+$ was used at ca. $1-5 \times 10^{-5}$ mol dm^{-3}, and all ReAZBAP$^+$-H$^+$ and -M^{n+} samples were at [H$^+$] or [M^{n+}] $\approx$ 0.1 mol dm^{-3}, except for studies of concentration dependence, to minimize the proportion of noncomplexed ReAZBAP$^+$.

UV−vis absorption spectra were recorded using a Hitachi U-3000 spectrophotometer with matched quartz cells of 1 mm or 1 cm path length. Corrected emission and excitation spectra were recorded using a Jobin-Yvon FluoroMax-2 spectrofluorimeter with right-angle collection geometry and a 1 cm path length quartz cell, with quantum yields measured versus (bpy)Re(CO)$_3$Cl in acetonitrile ($\Phi_{em} = 0.005$)[53] as reference. The experimental and analytical methods for nanosecond TRVIS and emission studies have been described previously:[52] degassed samples ($\geq$3 freeze−pump−thaw cycles) were contained in cells of 1.0 cm path length, and at a RaAZBAP$^+$ concentration that gave an absorbance of $A \approx 0.5$ at the excitation wavelength of 355 nm (10 ns, 5−10 mJ).

The SPSS software package (SPSS Inc.) was used for nonlinear regression analysis, and uncertainties are quoted as 95% confidence limits ($\pm 2\sigma$). Kinetic data were fitted either using SPSS at times outside the instrument response function, or using in-house software that enabled analysis at all times by convolution of the model expression with the instrument response function; lifetimes ($\tau = 1/k$) were obtained with uncertainties of $\pm$5−10%.

Results and Discussion

Steady-state and nanosecond time-resolved UV−vis absorption and emission studies were carried out on ReAZBAP-Li$^+$, -Na$^+$, -K$^+$, -Mg^{2+}, -Ca^{2+}, and -Ba^{2+} in acetonitrile. The steady-state data are presented first, and the time-resolved data are then presented sequentially, at increasing time scales after excitation,

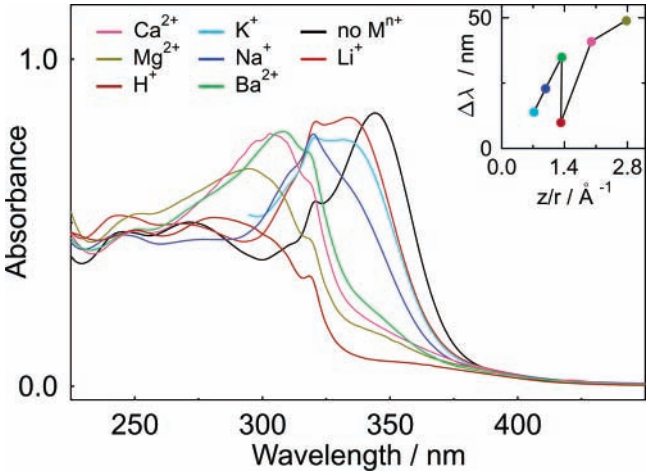

Figure 1. UV−vis absorption spectra of ReAZBAP$^+$ (1×10^{-5} mol dm^{-3}), ReAZBAP-H$^+$ formed on addition of HCl (0.1 mol dm^{-3}), and ReAZBAP$^+$-M^{n+} formed on addition of metal salts ([M^{n+}] ≈ 0.1 mol dm^{-3}); spectrum from the KNCS sample edited at <300 nm because of strong absorption by the thiocyanate ion. Inset: hypsochromic shift on complexation ($\Delta\lambda$) vs cation charge-to-radius (z/r) ratio.

TABLE 1: UV−Vis Absorption, Emission, and Binding Constant Data for ReAZBAP$^+$ and Its M^{n+} Complexes in Acetonitrile[a]

cation	λ_{max}	ϵ_{max}	log K	τ_{em}	Φ_{em}
none	344	42000		<1	0.0035
Li^+	334	41500	2.0 ± 0.3	12	0.0055
Na^+	321	38000	1.8 ± 0.1	10	0.0042
K^+	330	38000	1.4 ± 0.4	<1[b]	0.0012[b]
Mg^{2+}	295	33500	1.4 ± 0.4	140	0.0470
Ca^{2+}	303	38500	2.6 ± 0.1	56	0.0130
Ba^{2+}	309	39500	2.1 ± 0.2	47	0.0087
H^+	281	26000		140	0.0280

[a] Band positions in nm, absorption coefficients in dm^3 mol^{-1} cm^{-1}, log binding constants in dm^3 mol^{-1}, and emission lifetimes in ns. [b] Values affected by reaction with SCN$^-$ counterion (see Supporting Information).

to describe each of the individual processes that combine to form the complete ion release-and-recapture cycles.

UV−Vis Absorption Spectroscopy: Metal Cation Binding. The UV−vis absorption spectrum of ReAZBAP$^+$ in acetonitrile (Figure 1) shows an intense band at $\lambda_{max} = 344$ nm, which has been assigned to an intraligand charge-transfer (ILCT) transition in which charge is transferred from the azacrown electron donor to the amidopyridyl electron acceptor; a weaker MLCT band at $\lambda_{max} \approx 350$ nm underlies it.[46,52] The addition of acid to form ReAZBAP$^+$-H$^+$, or of metal salts to form ReAZBAP$^+$-M^{n+}, results in a blue-shift in the ILCT band (Figure 1 and Table 1; Figure S1 in Supporting Information), with the largest shift occurring on protonation. Such shifts are well-documented for chromophores linked to azacrown ethers,[23−25,31,36,54] and they are attributed to the interaction of the cation with the azacrown nitrogen atom increasing its oxidation potential,[46] raising the energy of the ILCT transition, and giving a shift in peak wavelength ($\Delta\lambda$) whose magnitude correlates broadly with the charge-to-radius[55] (z/r) ratios of the cations (Figure 1, inset). An obvious anomaly in the general trend is Li^+ that, despite its high z/r ratio, gives a small shift that has been attributed to this small cation binding to the four azacrown oxygen atoms and remaining relatively remote from the azacrown N-atom.[36,56,57] Both this effect and the overall trend have been observed generally for other chromophores attached to aza-15-crown-5 ethers.

UV−vis titration experiments provided cation binding constants K (eq 1) by fitting the absorbance at 344 nm to eq 2,[54] where A_0, A, and A_∞ are the absorbances in the absence of M^{n+}, in the presence of M^{n+}, and in the limiting case of full cation binding, respectively, and the total ligand and total metal concentrations are $[L]_{tot} = [L] + [LM^{n+}]$ and $[M^{n+}]_{tot} = [M^{n+}] + [LM^{n+}]$, respectively.

$$\text{ReAZBAP}^+ + M^{n+} \overset{K}{\rightleftharpoons} \text{ReAZBAP}^+\text{-}M^{n+} \quad (1)$$

$$A = A_0 + \frac{(A_\infty - A_0)}{2[L]_{tot}}\left([L]_{tot} + [M^{n+}]_{tot} + \frac{1}{K} - \sqrt{\left([L]_{tot} + [M^{n+}]_{tot} + \frac{1}{K}\right)^2 - 4[L]_{tot}[M^{n+}]_{tot}}\right) \quad (2)$$

Clear isosbestic points and good fits to eq 2 indicated that 1:1 binding occurs (Figure S1), and the measured K values are given in Table 1.[58] The binding constants obtained for ReAZBAP$^+$ are low within the range of values reported for these respective metal cations with other aza-15-crown-5 chromophores;[23,36,54,57,59,60] this effect is attributable to an azacrown N-atom that carries a partial positive charge as a result of its linkage to an electron-accepting Re^I group within the positively charged ReAZBAP$^+$. The variation in the magnitude of K with metal cation does not correlate with the bandshifts, as is also reported for other azacrown sensors, but the trend observed here is similar to that for other aza-15-crown-5 systems;[36,51,61] it has been rationalized through a combination of several effects including size-matching between azacrown and cation, cation desolvation thermodynamics, and the nature of the interaction between these hard cations and the hard oxygen and soft nitrogen atoms of the azacrown.[62]

UV−Vis Emission Spectroscopy: MLCT Excited-State Kinetics. The 355 nm excitation of ReAZBAP$^+$ and its -H$^+$ and -M^{n+} complexes gives emission at $\lambda_{max} \approx 600$ nm that is assigned to the MLCT excited state.[46,52] The emission from ReAZBAP$^+$ is very weak and has a short lifetime of $\tau_{em} < 1$ ns due to rapid quenching of the MLCT state by electron transfer to form the LLCT state, with $\tau_{FET} = 500$ ps (Scheme 2).[46,52,63,64] The emission quantum yield and lifetime increase on forming the ReAZBAP$^+$-H$^+$ and -M^{n+} complexes (Figure 2; Table 1)[65] and the emission kinetics fit well to a single exponential decay in all cases. Protonation substantially increases the MLCT emission yield and lifetime to that of ReBAP$^+$ by raising the energy of the LLCT state so that effectively all of the photophysics occurs via the MLCT state.[52] The ReAZBAP$^+$-Li^+, -Na^+, -Ca^{2+}, and -Ba^{2+} complexes give MLCT emission yields and lifetimes that are intermediate between the two limiting cases of ReAZBAP$^+$ and ReAZBAP$^+$-H$^+$, indicating that the extent of quenching via the LLCT state decay route depends on the identity of the metal cation;[46] the radiative lifetime also appears to vary.[46,66] ReAZBAP$^+$-Mg^{2+} gives an emission lifetime that is similar to that of the protonated complex, indicating that the MLCT state is not quenched in this case. The ReAZBAP$^+$-K^+ sample gave a very low emission yield and short lifetime that we attribute to reactive quenching of the MLCT state by the thiocyanate counterion (see Supporting Information); no further studies were carried out on this sample.

TRVIS Spectra at <50 ns: Observation of Excited States. TRVIS spectra of all the ReAZBAP$^+$-M^{n+} complexes were recorded on 355 nm excitation (Figure 2).[67] A comparison of the TRVIS spectra of ReAZBAP$^+$-Li^+, -Na^+, -Mg^{2+}, -Ca^{2+}, and -Ba^{2+} at short time delays with those of ReAZBAP$^+$-H$^+$ [52] and ReAZBAP$^+$ (Figure 3) indicates that the transient spectrum

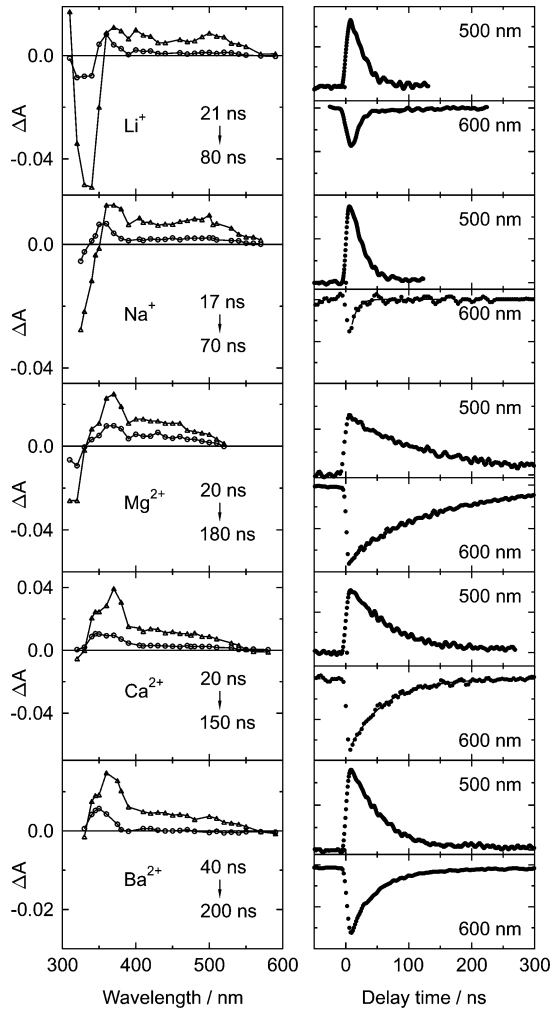

Figure 2. TRVIS spectra (left) obtained on 355 nm excitation of the ReAZBAP$^+$-M^{n+} complexes in acetonitrile, with delay times as indicated. Corresponding kinetics (right) as monitored by UV−vis absorption (upper in each case) and emission (lower in each case), with probe wavelengths as indicated. Solid lines show fits to the emission data (Table 1).

may be attributed in each case predominantly to either the MLCT or the LLCT excited state.

The TRVIS spectra of ReAZBAP$^+$-Mg^{2+}, -Ca^{2+}, and -Ba^{2+} at <50 ns (Figure 2) show a bleach at <330 nm,[67] along with a sharp absorption band at ca. 370 nm and a weak, broad absorption at ca. 400−550 nm (Figure 3 left). These spectra are similar to the TRVIS spectrum of ReAZBAP$^+$-H^+, which has been assigned to the MLCT state,[52] with the band at 370 nm assigned specifically to its bpy•$^-$ component.[53] The TRVIS spectra of ReAZBAP$^+$-Li^+ and -Na^+ at <30 ns (Figure 2) show a bleach at <360 nm that is red-shifted from that of the ReAZBAP$^+$-M^{2+} systems because of a red-shift in the ground-state spectra (Figure 1) and absorption at ca. 370 nm that may be distorted by the strong bleach; in addition, they show a band peaking at 500 nm (Figure 3, right). These spectra are similar to the ns-TRVIS spectrum of ReAZBAP$^+$ (Figure 3, right), which has been assigned to the LLCT state.[52] The absorption at ca. 370 nm is again assigned to the bpy•$^-$ component, and the additional band at 500 nm is assigned to the NR_2•$^+$ component formed on electron transfer (Scheme 2),[52] which overlies any bpy•$^-$ absorption in this region; the very strong bleach at <360 nm corresponds to loss of the intense ILCT absorption band (Figure 1) and is also consistent with oxidation of the azacrown N-atom in the LLCT state.

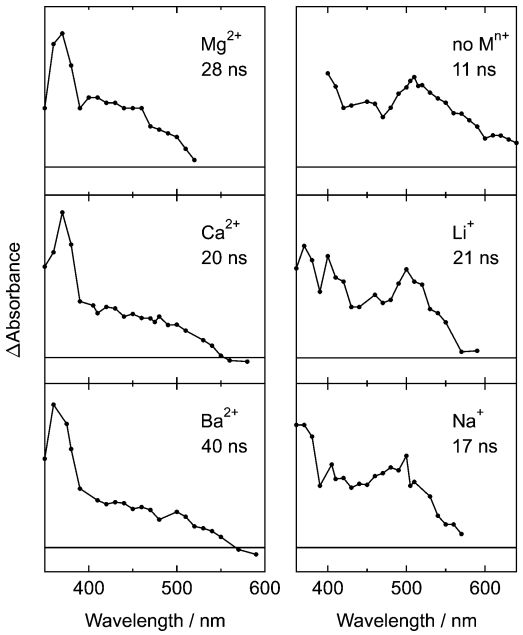

Figure 3. TRVIS spectra recorded at <50 ns after 355 nm excitation of ReAZBAP$^+$-M^{n+}, with delay times as indicated.

TRVIS Spectra at ca. 50−200 ns: Observation of Ion Release. The TRVIS spectra of ReAZBAP$^+$-Li^+, -Na^+, -Ca^{2+}, and -Ba^{2+} decay to the baseline without a discernible change in profile at ≥400 nm, but the profiles at <400 nm change with delay time. A partial recovery of the bleach and a partial decay of the band at ca. 370 nm occur concurrently, and on a different time scale for each metal cation, but the Δ*A* signal does not approach the baseline immediately for any of these samples: a distinct positive absorption band at ca. 350 nm and a residual bleach at shorter wavelength[67] are evident at ≳70 ns (Figure 2).

A specific spectroscopic signature for ion release is obtained for each metal cation by subtracting the respective steady-state UV−vis spectrum of a ReAZBAP$^+$-M^{n+} sample from that of the metal-free ReAZBAP$^+$ sample at the same concentration. The TRVIS profiles observed from ReAZBAP$^+$-Li^+, -Na^+, -Ca^{2+}, and -Ba^{2+} at ca. 50−200 ns, with the appropriate delay time depending on the metal cation, closely match these respective signatures for ion release, as shown in Figure 4, demonstrating clearly that these ions are released and that ground-state ReAZBAP$^+$ is generated within ≲50−200 ns of photoexcitation.

The TRVIS spectrum of ReAZBAP$^+$-Mg^{2+}, like that of ReAZBAP$^+$-H^+, decays without any change in profile across the whole probe wavelength range, and it does not match the signature for ion release at any delay time. Thus, the evidence indicates that Mg^{2+} is not released on photoexcitation.

Kinetics and Mechanism of Ion Release. The TRVIS kinetics observed at early times on excitation of ReAZBAP$^+$-Li^+, -Na^+, -Mg^{2+}, -Ca^{2+}, and -Ba^{2+} vary between those reported previously for ReAZBAP$^+$, where the LLCT state is observed with lifetime $\tau_{LLCT} = 19$ ns, and ReAZBAP$^+$-H^+, where the MLCT state is observed with lifetime $\tau_{MLCT} = 140$ ns.[52] For ReAZBAP$^+$-M^{n+}, the TRVIS kinetics at 500 nm show an instrument-limited rise-time followed by a decay to the baseline with a lifetime of $\tau \leq 140$ ns that depends on the identity of the cation; both the MLCT and the LLCT excited states absorb at 500 nm, and the kinetics observed at this wavelength may be attributed to these states.

SCHEME 3: General Photochemical Mechanism for ReAZBAP$^+$-M^{n+}

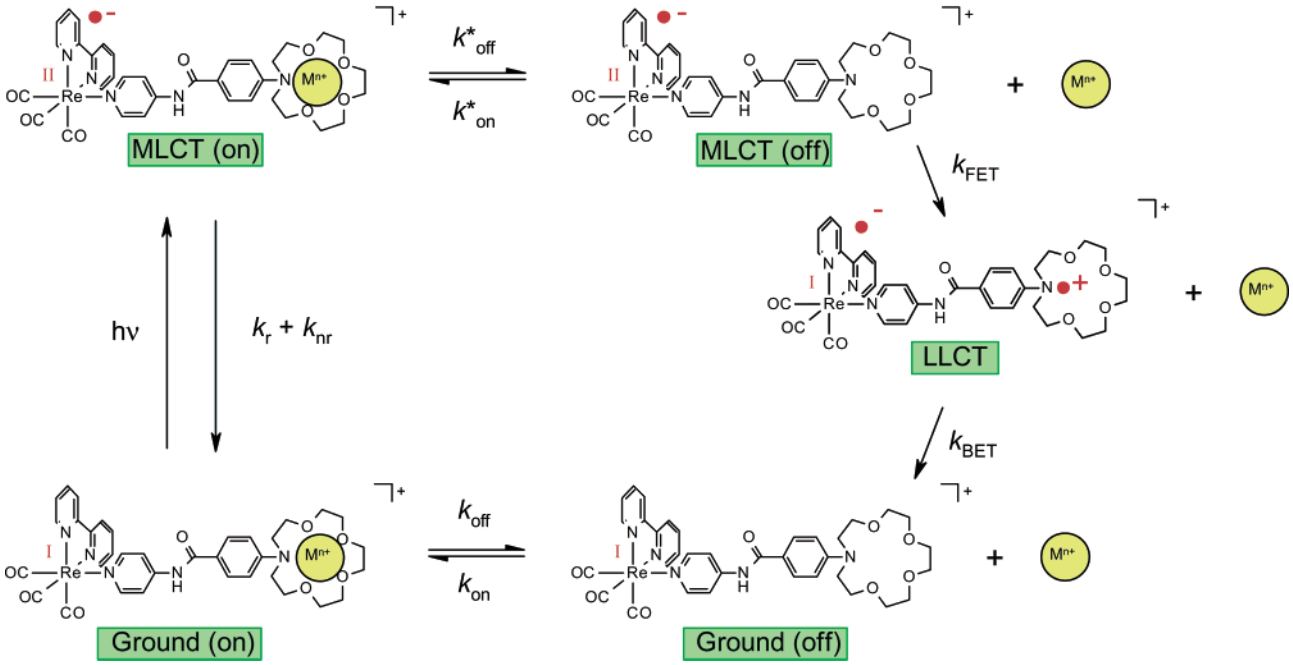

The TRVIS kinetics of ReAZBAP$^+$-Mg^{2+} fit well to a monoexponential decay with a lifetime of 140 ns, which matches that obtained from the emission kinetics. Therefore, all of the data for this metal cation are consistent with the observation of only the MLCT excited state and with the conclusions that Mg^{2+} is not released and that the LLCT state does not form. This interpretation is also consistent with the conclusion from electrochemical studies that electron transfer to form the LLCT state is energetically unfavorable and does not occur when a metal cation is bound to the azacrown.[46]

The TRVIS kinetics of ReAZBAP$^+$-Li$^+$, -Na$^+$, -Ca^{2+}, and -Ba^{2+} at 500 nm are all slower than the respective MLCT emission kinetics (Figure 2), indicating that the absorption arises not only from the MLCT state but also from a longer-lived state.

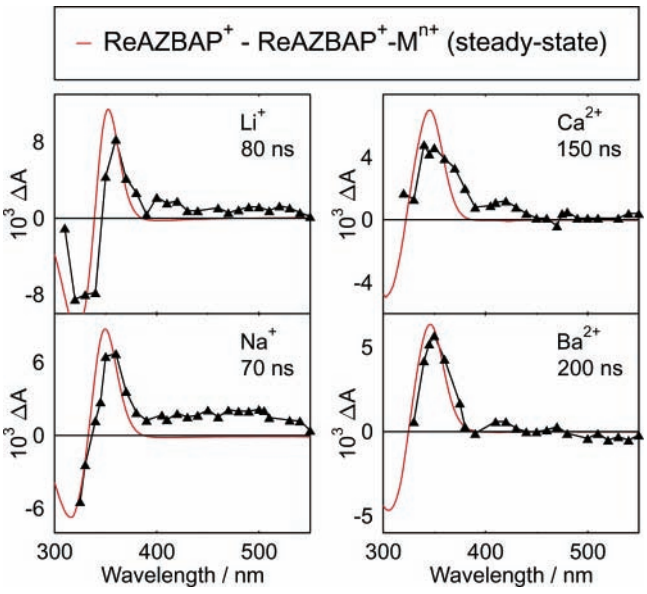

Figure 4. TRVIS spectra recorded at ca. 50−200 ns after 355 nm excitation of ReAZBAP$^+$-M^{n+}, with delay times as indicated, overlaid with the difference spectra obtained by subtracting the steady-state UV−vis spectrum of the respective ReAZBAP$^+$-M^{n+} complex from that of ReAZBAP$^+$.

The observation of a clear signature for ion release in each case enables this longer-lived state to be assigned as the LLCT state, which forms rapidly from the MLCT state (Scheme 2) after the metal cation is released from the azacrown. The TRVIS kinetics of ReAZBAP$^+$-Li$^+$ and -Na$^+$ are fast but slower than those of ReAZBAP$^+$: they may be attributed to fast ion release, so that the LLCT state is produced rapidly and dominates the TRVIS kinetics, as it does the TRVIS spectra (Figure 3 right). By contrast, the TRVIS kinetics of ReAZBAP$^+$-Ca^{2+} and -Ba^{2+} are relatively slow, although faster than those of ReAZBAP$^+$-H$^+$: they may be attributed to relatively slow ion release, so that the decay of the MLCT state dominates the TRVIS kinetics, as it does the TRVIS spectra (Figure 3 left).

Scheme 3 shows a general mechanism for ion release[46] that we have used as the basis for quantitative analysis by fitting the TRVIS kinetics at 500 nm to a kinetic model using the rate constants and the relative absorption coefficients for each of the excited states in this scheme as parameters. Values obtained from our earlier studies in the absence of metal cations[52] are fixed in the fit as follows, where MLCT(on) and MLCT(off) correspond to the MLCT excited state with a metal cation bound and absent, respectively. The rate constant for nonreactive decay of the MLCT(on) excited state, via radiative and nonradiative routes, is set to that obtained from the emission lifetime of ReBAP$^+$ as $(k_r + k_{nr}) = 6.9 \times 10^6\ s^{-1}$.[68] The rate constant for forward electron transfer from MLCT(off) to LLCT states is set to $k_{FET} = 2 \times 10^9\ s^{-1}$, and the rate constant for back electron transfer from LLCT to ground states is set to $k_{BET} = 5.3 \times 10^7\ s^{-1}$, as measured previously for ReAZBAP$^+$ in the absence of metal cations. The absorption coefficients of the MLCT and LLCT states are significantly different at 500 nm, and the ratio of $\epsilon_{MLCT(off)} = 0.6\epsilon_{LLCT}$ is set to that obtained from ultrafast TRVIS spectra of ReAZBAP$^+$; it is assumed that $\epsilon_{MLCT(on)} = \epsilon_{MLCT(off)}$. It is also assumed that $k_{FET} \gg k^*_{on}$ (i.e., that ion rebinding in the MLCT(off) state is not competitive with its rapid decay to the LLCT state (Scheme 2)), and so k^*_{on} is not included in the kinetic model. Thus, all of the parameters are fixed except k^*_{off}, which is obtained by an iterative fit of the kinetic model to the experimental data. In the case of

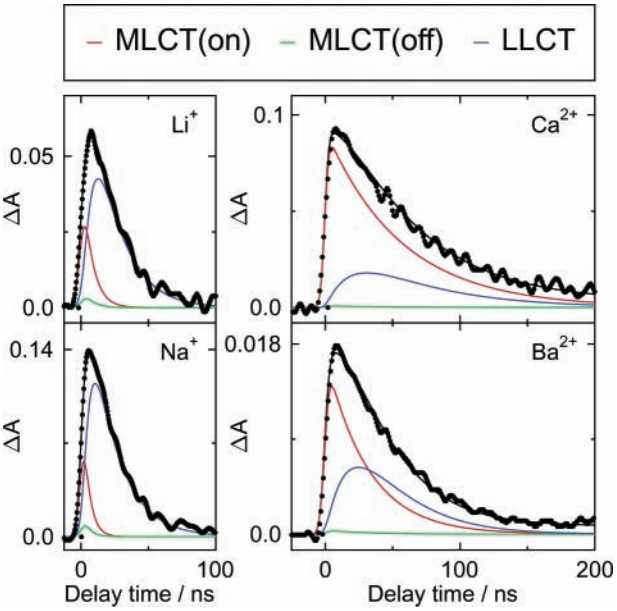

Figure 5. TRVIS kinetics recorded at 500 nm on 355 nm excitation of ReAZBAP$^+$-M^{n+}, overlaid with a kinetic fit to Scheme 3 (see text) showing the total fitted ΔA signal and the contributions from the MLCT(on), MLCT(off), and LLCT states.

TABLE 2: Rate Constants for Excited-State Cation Release from ReAZBAP$^+$ Obtained from Fitting TRVIS Kinetics at 500 nm to Scheme 3 (See Text)

cation	k^*_{off}/s^{-1}
Li^+	1.25×10^8
Na^+	1.67×10^8
Ca^{2+}	1.12×10^7
Ba^{2+}	2.50×10^7

ReAZBAP$^+$-Ca^{2+} and -Ba^{2+}, a small positive ΔA offset due to a permanent photoproduct (see below) is also included in the fit.

This analysis fits the data well: Figure 5 shows the experimental data, the total ΔA values obtained from the fit, and the time-dependent contributions to this total from each of the MLCT(on), MLCT(off), and LLCT states. In all cases, the MLCT(off) state gives a very small contribution to the total signal because the rate constant for its decay to the LLCT state ($k_{FET} = 2 \times 10^9$ s^{-1}) is significantly higher than the rate constant for its formation, $k^*_{off} \approx 2-17 \times 10^7$ s^{-1}, as determined by the fit and given in Table 2. The overall transient absorbance is therefore dominated by contributions from the MLCT(on) and LLCT states, as shown in Figure 5.

The high values of $k^*_{off} = 1.25 \times 10^8$ and 1.67×10^8 s^{-1} obtained for Li^+ and Na^+, respectively, show that these ions are released rapidly on photoexcitation, with $\tau^*_{off} = 8$ and 6 ns, respectively. These values are consistent with all of the experimental data, including MLCT emission with a low yield and short lifetime (Table 1; Figure 2) and TRVIS spectra (Figure 3, right) and kinetics (Figure 5) that are dominated by the LLCT state formed after ion release.

The relatively low value of $k^*_{off} = 1.12 \times 10^7$ s^{-1} obtained for Ca^{2+} shows that this ion is released relatively slowly, with $\tau^*_{off} = 89$ ns. Again, this is consistent with all of the experimental data, including MLCT emission with a relatively high yield and long lifetime (Table 1; Figure 2) and TRVIS spectra (Figure 3 left) and kinetics (Figure 5) that are dominated by the MLCT state because ion release is the rate-determining step for decay to the ground state in this case; the LLCT state does not dominate at any delay time. The value of $k^*_{off} = 2.50 \times 10^7$ s^{-1} obtained for Ba^{2+} indicates that it is released with $\tau^*_{off} = 40$ ns; this is more rapidly than Ca^{2+} but much more slowly than Li^+ and Na^+, consistent with experimental data that are intermediate between these cases and that are most comparable to those from Ca^{2+}.

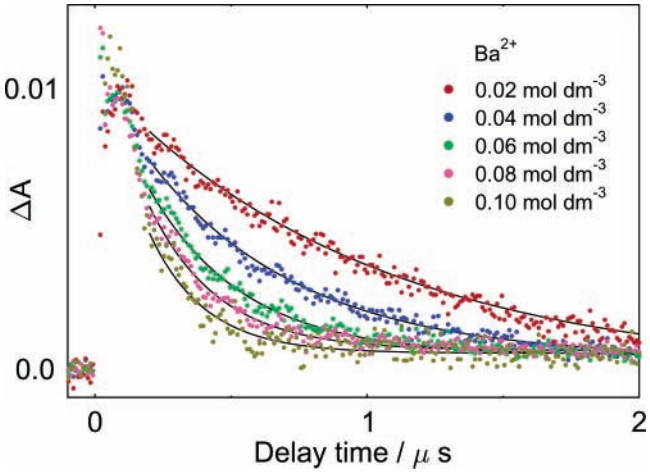

Figure 6. TRVIS kinetics recorded at 345 nm on 355 nm excitation of ReAZBAP$^+$-Ba^{2+} as a function of Ba^{2+} concentration, overlaid with fits to a single-exponential decay with offset at delay times of >200 ns (i.e, after decay of the excited states).

These studies firmly establish the general mechanism for ion release in the ReAZBAP$^+$ system by direct observation of the states in Scheme 3, and they quantify the specific rate constants that depend on the identity of the metal cation. Our observations fully support the excited-state release mechanism first proposed by MacQueen and Schanze on the basis of indirect MLCT emission studies.[46]

TRVIS Studies at ca. 0.2−500 μs: Observation of Ion Recapture. The TRVIS bands at ca. 350 nm, which are assigned to ground-state ReAZBAP$^+$ formed after ion release from ReAZBAP$^+$-Li$^+$, -Na$^+$, -Ca^{2+}, and -Ba^{2+} (Figure 4), decay over a markedly longer time scale than the excited-state bands at >400 nm. The remaining ΔA signal decays almost to the baseline in each case, indicating that the dominant pathway results in a return to the starting equilibrium through metal cation recapture. The TRVIS kinetics at ca. 350 nm fit well to a monoexponential decay at delay times longer than those required for the complete decay of the respective absorption at >400 nm: the observed rate constants for cation recapture, k_{obs}, show a strong dependence on the bulk concentration of metal cation (Figure 6), giving observed lifetimes in the range $\tau_{obs} = 0.1-10$ μs. Both the time scale and the M^{n+} concentration dependence indicate that the ions are recaptured from bulk solution rather than geminately, providing further confirmation that Li^+, Na^+, Ca^{2+}, and Ba^{2+} are released into bulk solution on photoexcitation of the ReAZBAP$^+$-M^{n+} complex.

For ReAZBAP$^+$-Ca^{2+} and -Ba^{2+}, the TRVIS spectrum of metal-free ReAZBAP$^+$ decays directly to the final baseline as ReAZBAP$^+$-M^{n+} re-forms. For ReAZBAP$^+$-Li$^+$ and -Na$^+$, however, the starting equilibrium does not reestablish directly as the TRVIS spectrum of ReAZBAP$^+$ decays: it does so via a further intermediate that is characterized by a TRVIS profile at ca. 1−100 μs that consists mainly of a bleach peaked at 330 nm, and that closely matches the respective difference spectrum obtained by subtracting the steady-state UV−vis spectrum of ReAZBAP$^+$-Li$^+$ or ReAZBAP$^+$-Na$^+$ from that of ReAZBAP$^+$-H$^+$, as shown in Figure 7. The similarity of the observed difference spectra with those that would be obtained by protonation indicates that Li^+ and Na^+ associate initially with

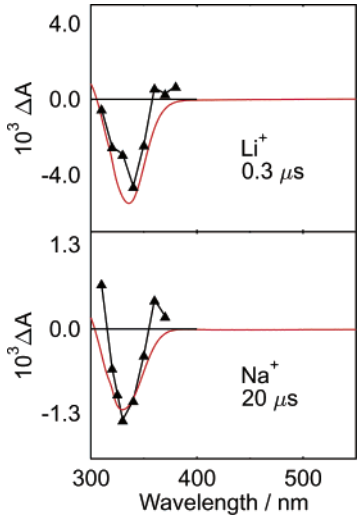

Figure 7. TRVIS spectra recorded at 0.3 and 20 μs after 355 nm excitation of ReAZBAP$^+$-Li$^+$ and -Na$^+$, respectively, overlaid with the difference spectra obtained by subtracting the steady-state UV−vis spectrum of the respective ReAZBAP$^+$-M^{n+} complex from that of ReAZBAP$^+$-H$^+$.

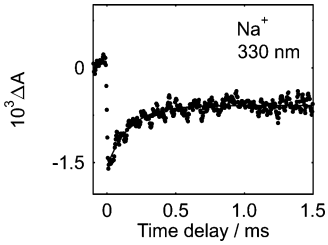

Figure 8. TRVIS kinetics recorded at 330 nm on 355 nm excitation of ReAZBAP$^+$-Na$^+$, overlaid with a fit to a single-exponential decay with offset at delay times of >10 μs.

the azacrown N-atom before adopting their equilibrium positions within the azacrown cavity. This bleach at 330 nm shows a monoexponential decay with a lifetime of $\tau'_{obs} \approx 150$ μs (Figure 8), which is relatively insensitive to metal cation concentration over the limited range of [M^{n+}] $\approx$ 0.1 mol dm^{-3} at which these very weak features could be measured.

Kinetics and Mechanism of Ion Recapture. The ion recapture process occurs in the ground electronic state (i.e., after excited-state decay (Scheme 3)). Hence, this measurement is one of a sample relaxing to its thermal equilibrium: the pulse of light causes a jump in the metal-free ReAZBAP$^+$ concentration, which shifts the position of the equilibrium, and the long-time TRVIS data record the relaxation to the starting equilibrium (Scheme 4).

The decay of the TRVIS spectrum assigned to metal-free ReAZBAP$^+$ gives observed first-order rate constants, k_{obs}, which show a linear dependence on [M^{n+}]. This is consistent with the

SCHEME 4: General Mechanism for the Relaxation of a Light-Induced ReAZBAP$^+$-M^{n+} Concentration Jump

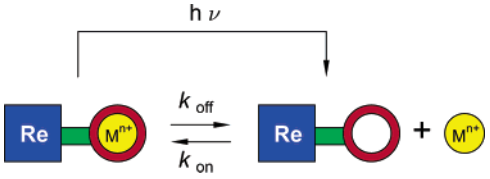

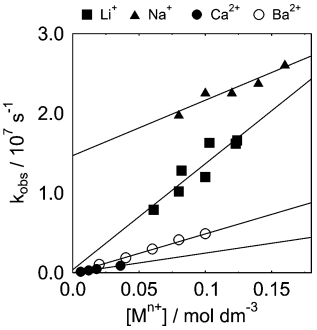

Figure 9. Plots of k_{obs}, obtained from single-exponential fits to TRVIS kinetics recorded at 345−350 nm on 355 nm excitation of ReAZBAP$^+$-M^{n+} vs M^{n+} concentration; linear fits are overlaid.

TABLE 3: Rate Constants for Ground-State Cation Binding to ReAZBAP$^+$ Obtained from a Direct Analysis of the Data According to Scheme 4, along with Measured Values of *K*

cation	k_{on}/dm^3 mol^{-1} s^{-1}	k_{off}/s^{-1}	k'_{obs}[a]/s^{-1}	(k_{on}/k_{off})/ dm^3 mol^{-1}	K/ dm^3 mol^{-1}
Li^+	1.3×10^8	$\leq 7 \times 10^6$	6.2×10^3	≥ 19	112
Na^+	6.9×10^7	1.5×10^7	5.3×10^3	4.6	66
Ca^{2+}	2.5×10^7	$\leq 8 \times 10^4$		≥ 310	440
Ba^{2+}	5.0×10^7	$\leq 4 \times 10^5$		≥ 125	132

[a] Measured at [Li^+] = 0.10 and [Na^+] = 0.09 mol dm^{-3}; $k'_{obs} = 6.3 \times 10^3$ s^{-1} for [Na^+] = 0.18 mol dm^{-3}.

simple mechanism in Scheme 4, which may be analyzed by eq 3 in accordance with standard relaxation kinetics.

$$k_{obs} = k_{on}[M^{n+}] + k_{off} \quad (3)$$

Fits to eq 3 are shown in Figure 9, with the fitted rate constants given in Table 3. The values obtained for k_{on} are similar for all the metal cations and are in the range of (2−13) $\times 10^7$ dm^3 mol^{-1} s^{-1}. By contrast, the values obtained for k_{off} are quite different for the different metal cations, with a value of 1.5×10^7 s^{-1} obtained for Na^+ and those for the remainder being too small to measure accurately but with limiting values in the range of $\leq$(8−700) $\times 10^4$ s^{-1}.

The kinetics assigned to a metal cation relocating from the azacrown N-atom to its equilibrium position within the azacrown, observed here only for Li^+ and Na^+, give observed first-order rate constants of $k'_{obs} \approx 6 \times 10^3$ s^{-1} at the concentrations studied (Table 3). The observation of a multistep binding process for Li^+ and Na^+, and a discrepancy between the binding constants measured spectrophotometrically and those estimated from the observed rate constants as k_{on}/k_{off} (Table 3), indicates that the mechanism for these cations is more complicated than that given by Scheme 4.

Scheme 4 gives a phenomenological interpretation of the data. They may interpreted alternatively in terms of the general Eigen−Winkler mechanism shown in Scheme 5,[69−74] which considers the binding of cations to macrocycles as a sequential multistep process: the cation initially forms a contact pair with the macrocycle; it then forms an exclusive complex in which the cation is external to the cavity; and, finally, solvent molecules in the cation coordination sphere are replaced by

SCHEME 5: General Mechanism for Cation Binding to Crown Ethers

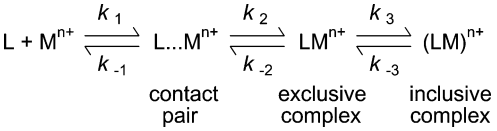

TABLE 4: Rate Constants for Ground-State Cation Binding to ReAZBAP$^+$ Obtained from an Interpreted Analysis of the Data According to Schemes 5 (Li^+, Na^+) or 6 (Ca^{2+}, Ba^{2+}), along with Measured Values of *K*

cation	scheme	K_1/dm^3 mol^{-1}	k_2/s^{-1}	k_{-2}/s^{-1}	K_2[a]	K_3[b]	k_3/s^{-1}	k_{-3}/s^{-1}	K/dm^3 mol^{-1}
Li^+	5	0.10	1.3×10^9	$\leq 7 \times 10^6$	≥ 190	≤ 6	$\leq 1 \times 10^4$	$\leq 2 \times 10^3$	112
Na^+	5	0.12	5.8×10^8	1.5×10^7	38	14	1.6×10^4 [d]	1.1×10^3 [d]	66
Ca^{2+}	6	0.12	2.1×10^8	$\leq 8 \times 10^4$	≥ 2600[c]				440
Ba^{2+}	6	0.17	2.9×10^8	$\leq 4 \times 10^5$	≥ 735[c]				132

[a] Calculated from $K_2 = k_2/k_{-2}$. [b] Calculated from $K = K_1K_2K_3$. [c] If K_2 is calculated from $K = K_1K_2$, then: $K_2 = 3700$ and $k_{-2} = 5.7 \times 10^4$ s^{-1} for Ca^{2+}, and $K_2 = 780$ and $k_{-2} = 3.7 \times 10^5$ s^{-1} for Ba^{2+}. [d] Average values from data reported in Table 3.

coordinating atoms of the macrocycle to form the fully bound inclusive complex. The overall binding constant, K (eq 1), is dependent on these three equilibria, as given by eq 4, where K_n are the equilibrium constants for the three individual steps 1−3 in Scheme 5.

$$K = K_1K_2K_3 \tag{4}$$

The first equilibrium in Scheme 5, the formation of a contact pair in which the metal cation and azacrown are separated by solvent, is established rapidly and on a shorter time scale than the observed ion recapture kinetics. We do not observe a distinct TRVIS signature of the contact pair, which may be expected to be similar to that of the metal-free complex, on rebinding of any of the cations; hence, the presence of this intermediate is inferred.

The Fuoss equation[75] can be used to estimate K_1 (dm^3 mol^{-1}) by eq 5,[72,73,76,77] where N_A is the Avogadro constant, a is the interionic distance of the contact pair (cm), and δ quantifies the electrostatic interaction between the ion and azacrown.

$$K_1 = \frac{4\pi N_A a^3}{3000} e^{-\delta} \tag{5}$$

If it is assumed that the azacrown is essentially uncharged due to the large distance between it and the Re center, then $\delta = 0$. The interionic distances are estimated as the sum of the azacrown ether radius, taken as 1 Å,[78] and the solvated ionic radii of 2.36, 2.62, 2.60, and 3.09 Å for Li^+, Na^+, Ca^{2+}, and Ba^{2+}, respectively, are taken by adding 1.6 Å to the crystallographic ionic radii,[55] to account for the solvation sphere.[76] Substituting these values into eq 5 gives estimated values of $K_1 = 0.10-0.17$ dm^3 mol^{-1} for these cations, as listed in Table 4.

The second and third equilibria in Scheme 5, corresponding to formation of the exclusive and inclusive complexes, respectively, are generally established more slowly than the first equilibrium. The distinct intermediates observed in the binding of Li^+ and Na^+ to ReAZBAP$^+$ provide good evidence for the applicability of Scheme 5: the TRVIS spectra assigned to Li^+ and Na^+ associated with the azacrown N-atom can be attributed to exclusive complexes, and the TRVIS kinetics on ca. 100 ns (τ_{obs}) and 100 μs (τ'_{obs}) time scales can be attributed to the respective relaxations as the exclusive and inclusive complexes form. Thus, for recapture of Li^+ and Na^+ by ReAZBAP$^+$, the observations indicate that the relative magnitudes of the rate constants are $k_1,k_{-1} \gg k_2,k_{-2} \gg k_3,k_{-3}$, with the first relaxation unobserved. In this case, and where $[M^{n+}] \gg [\text{ReAZBAP}^+]$, the rate constant observed for the second relaxation, k_{obs}, is given by eq 6,[72,74,79,80]

$$k_{obs} = \frac{k_2K_1[M^{n+}]}{1 + K_1[M^{n+}]} + k_{-2} \tag{6}$$

which simplifies to eq 7 in the limit $K_1[M^{n+}] \ll 1$, which is applicable at the metal cation concentrations used for these studies.

$$k_{obs} = k_2K_1[M^{n+}] + k_{-2} \tag{7}$$

Thus, the observed linear dependence of k_{obs} on $[M^{n+}]$ indicates that eq 7 is applicable, with $k_{on} = k_2K_1$ and $k_{off} = k_{-2}$ by comparison with eq 3. This interpretation gives values of $k_2 = 1.3 \times 10^9$ and 5.8×10^8 s^{-1} and $k_{-2} \leq 7 \times 10^6$ and $= 1.5 \times 10^7$ s^{-1}, for Li^+ and Na^+, respectively, with the ratios of these rate constants yielding respective values of $K_2 \geq 190$ and $= 38$ (Table 4).

The relaxation of the third equilibrium for the binding of Li^+ and Na^+ to ReAZBAP$^+$ is given by eq 8 under the conditions of $k_1,k_{-1} \gg k_2,k_{-2} \gg k_3,k_{-3}$ and $[M^{n+}] \gg [\text{ReAZBAP}^+]$ that apply here.[79,80]

$$k'_{obs} = \frac{k_3K_1K_2[M^{n+}]}{1 + K_1[M^{n+}] + K_1K_2[M^{n+}]} + k_{-3} \tag{8}$$

It was not possible to define the dependence of k'_{obs} on $[M^{n+}]$ because this process could only be observed at $[M^{n+}] \approx 0.1$ mol dm^{-3}, which is needed to prepare a sample with the metal-complexed form dominant for Li^+ and Na^+, and because the k'_{obs} values measured at the limits of the available conentration range were within the uncertainty limits of each other. However, estimates of k_3 and k_{-3} can be obtained from single-point data. The measured values of K, the estimated values of K_1 (eq 5), and the values of K_2 obtained from the ratio of the rate constants (Table 4) can be substituted into eq 4 to give $K_3 \leq 6$ and $= 14$ for Li^+ and Na^+, respectively, as given in Table 4. Taking $K_3 = k_3/k_{-3}$ and substituting experimental concentrations and measured k'_{obs} values into eq 8, along with the estimated values of K_1 and K_2, results in estimated values of $k_3 \leq 1 \times 10^4$ s^{-1} and $k_{-3} \leq 2 \times 10^3$ s^{-1} for Li^+ and $k_3 = 1.6 \times 10^4$ s^{-1} and $k_{-3} = 1.1 \times 10^3$ s^{-1} for Na^+ (Table 4).

By contrast to Li^+ and Na^+, the TRVIS signature of an exclusive complex in which the metal cation attaches to the azacrown N-atom was not observed in the binding of Ca^{2+} and Ba^{2+} to ReAZBAP$^+$, indicating either that such intermediates do not form or that their TRVIS signatures are unobserved because their decay kinetics are much faster than those of Li^+ and Na^+. In this situation, our interpretation is based on Scheme 6, in which Scheme 5 is simplified to a two-step mechanism. An analysis of the data by eq 7, which again is applicable, yields the k_2 and limiting k_{-2} values reported in Table 4.

SCHEME 6: Simplifed Mechanism for Cation Binding to Crown Ethers

$$L + M^{n+} \underset{k_{-1}}{\overset{k_1}{\rightleftharpoons}} L...M^{n+} \underset{k_{-2}}{\overset{k_2}{\rightleftharpoons}} (LM)^{n+}$$

contact pair — inclusive complex

Overall, the analyses indicate that the rate constants for attachment of M^{n+} to the azacrown (k_{on} or k_2) have approximately the same value for the four cations studied but that the rate constants for release (k_{off} or k_{-2}) of Li^+, Ca^{2+}, and Ba^{2+} are significantly lower than that for release of Na^+. The overall equilibrium constant K is governed by more than one component equilibrium constant and its associated rate constants, but it appears that the magnitude of K_2 and specifically this rate constant for release (k_{off} or k_{-2}) is particularly important in controlling the magnitude of K for these cations. The overall time scale for cation recapture to regenerate the starting sample is significantly slower for Li^+ and Na^+ than for Ca^{2+} and Ba^{2+}, under comparable conditions, despite the slightly faster initial attachment of these cations to the azacrown. The time scale for full relaxation is governed by the slowest step in the process, and the participation of a relatively long-lived intermediate in which the cation is attached to the azacrown N-atom prior to insertion into the cavity, observed here for Li^+ and Na^+ but not for Ca^{2+} and Ba^{2+}, is important in controlling the time scale required for full M^{n+} recapture.

Our TRVIS studies of M^{n+} binding to $ReAZBAP^+$ can be compared with the few examples of reported kinetic data for related systems. For azacrowns, one TRVIS study gave values of $k_{on} = 4 \times 10^7$ dm^3 mol^{-1} s^{-1} and $k_{off} = 1 \times 10^6$ s^{-1} for binding of Ba^{2+} to a benzothiazolium styryl aza-15-crown-5,[14] and another TRVIS study gave a value of $k_{on} = 9 \times 10^7$ dm^3 mol^{-1} s^{-1} for binding of Sr^{2+} to a merocyanine aza-15-crown-5;[26] these results are comparable with the values reported here for $ReAZBAP^+$ (Table 3). A direct comparison is provided only by Ba^{2+}, which has a similar value of k_{on} but a lower value of k_{off} value for $ReAZBAP^+$ than for the benzothiazolium system;[14] this difference is consistent with the higher value of K for $ReAZBAP^+$ than for the benzothiazolium system, and with our previous suggestion (above) that the value of k_{off} is particularly important in controlling the value of the overall binding constant. For cryptands, stopped-flow studies have shown relaxations on the millisecond time scale for Na^+, K^+, Ca^{2+}, Sr^{2+}, and Ba^{2+} binding to cryptands 222 and 221 in water.[8,74,76,81] The observation of two relaxations has been reported in some cases,[8,76] with the first being attributed to the formation of an exclusive complex in which the cation is associated with a nitrogen atom but outside the cryptand cavity and the second being attributed to insertion of the cation into the cavity. Our observations of two relaxations in the binding of Li^+ and Na^+ to $ReAZBAP^+$ are comparable to these observations of cryptands, with the distinct TRVIS spectroscopic signatures of these species substantiating the interpretation for $ReAZBAP^+$. The higher rate constants for the azacrown than the cryptand may be attributable, at least in part, to the azacrown having a more open and accessible structure. Our methodology provides an alternative and more direct approach to the ultrasonic, infrared, and NMR line-shape analyses that have commonly been used to study to the relatively fast relaxation kinetics of crown ethers.[69−72]

TRVIS Studies at ca. 0.1−1 ms: Observation of a Degradation Product. A weak residual TRVIS spectrum comprising a weak bleach at <330 nm and a very weak absorption at 370 nm was present at long times after photolysis in all cases and is assigned to a small concentration of permanent degradation product.[82] Figure 10 illustrates the observation with a TRVIS spectrum of $ReAZBAP^+$-Ca^{2+} at 150 μs, along with the steady-state difference spectrum obtained by subtracting the UV−vis spectrum recorded after a TRVIS experiment from that recorded before it. This product was not observed on continuous irradiation at ca. 355 nm, and it is likely to result from a very small proportion of two-photon events during the TRVIS studies, due to the moderately high peak irradiance (≤1 MW cm^{-2}) of the excitation laser pulse.

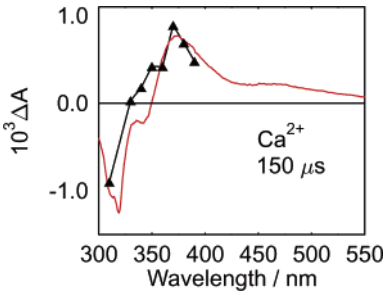

Figure 10. TRVIS spectrum recorded at 150 μs after 355 nm excitation of $ReAZBAP^+$-Ca^{2+}, overlaid with the difference spectrum obtained by subtracting a steady-state UV−vis spectrum of the $ReAZBAP^+$-Ca^{2+} sample after the TRVIS experiment from that recorded before it.

Comparison of Cation Binding in Ground and Excited States. The rate constants obtained for release of Li^+, Na^+, Ca^{2+}, and Ba^{2+} in the excited state (k^*_{off}; Table 2) show the same variation with metal cation as the ground-state binding constants, but they are all significantly higher than the respective rate constants for release in the ground state (k_{off} or k_{-2}; Tables 3 or 4). As discussed above, the magnitude of this rate constant for release appears to govern the overall binding constant in the ground state, and so the observed effect of light-controlled ion release may be attributed directly to a significant increase in its value on going to the MLCT excited state of $ReAZBAP^+$-M^{n+}. The increase in this rate constant may be attributed to the oxidation of Re^I to Re^{II} resulting in a redistribution of electron density that increases the partial positive charge at the azacrown N-atom; this indicates that there is effective electronic communication between these two centers, via the amide linker, although they are not in conjugation. This charge-transfer mechanism for lowering the binding constant in the excited-state applies to several all-organic cation probes,[22−26,28,29] where the charge-transfer state is formed on the group attached directly to the azacrown rather than on the more remote transition metal center in $ReAZBAP^+$. The absence of cation release from $ReAZBAP^+$-H^+ and -Mg^{2+} may be attributed to the strong interactions of these cations with the azacrown-N atom, as shown by the UV−vis data (Figure 1; Table 1). These strong interactions may be expected to lower the extent of charge transfer in the excited state, resulting in a rate constant for release in the excited state that is not increased significantly from that in the ground state and that does not compete with the sum of the rate constants for radiative and nonradiative decay of the MLCT(on) state to the ground state.

It should be noted that the excited-state release mechanism from $ReAZBAP^+$-M^{n+} may be different from the ground-state release mechanism because it occurs from a complex that has a different charge distribution in the excited state. The general mechanisms for thermal release in the ground state are given by the reverse reactions in Schemes 5 and 6. In the case of Li^+ and Na^+ (Scheme 5), the process involves association of the cation with the azacrown N-atom as partial solvation occurs prior to full release; release in the excited state may not involve cation attachment to the azacrown N-atom prior to full release because of its increased partial positive charge.

Following cation release in the excited state, free $ReAZBAP^+$ undergoes rapid electron transfer to form the LLCT state in 500 ps (Scheme 2),[52] in which a formally full positive charge at the azacrown N-atom may be expected to prevent M^{n+} geminate rebinding. The LLCT state lifetime of 19 ns[52] may be compared

with the distances that the released cations are estimated to travel during this time by eq 9,[25] where l is the mean diffusion length, D is the translational diffusion coefficient, and t is the time.

$$l = (2Dt)^{1/2} \quad (9)$$

The estimated distances of 63, 71, 55, and 57 Å travelled by Li^+, Na^+, Ca^{2+}, and Ba^{2+}, respectively,[83] indicate that the released cations diffuse a significant distance from the azacrown cavity, which has a diameter of ca. 2 Å,[78] while the complex remains in the LLCT state; they support the observations of full release into bulk solvent.

The LLCT state of $ReAZBAP^+$ is formed only via the MLCT(off) excited state and is not accessed directly by photon absorption; it is long-lived because the back electron-transfer reaction from the bpy to the amido-azacrown ligand, to re-form to the ground state, occurs in the Marcus inverted region.[52] Geminate ion rebinding that competes with release to bulk solvent is a general concern for all-organic designs because the charge-transfer states that may induce ion release are generally accessed directly by photon absorption, and they commonly undergo rapid back electron-transfer reactions that restore the ground-state charge distribution on a very short time scale. Hence, the LLCT state of $ReAZBAP^+$ may play an important role in facilitating full ion release to bulk solvent by providing a barrier to rebinding that persists for longer than the time scale required for the metal cations to diffuse away from the azacrown. The presence of an optically inaccessible and long-lived charge-separated state arises from incorporating a transition-metal redox center in the molecular design, and this feature may be advantageous in the generic design of light-controlled ion switches.

Conclusions

We have demonstrated conclusively that $ReAZBAP^+$ acts as a light-controlled ion switch of Li^+, Na^+, Ca^{2+}, and Ba^{2+}. We have made direct observations of the excited states involved in cation release, and we have determined the rate constants for each step for these four cations. We have observed the thermal process of cation rebinding to $ReAZBAP^+$, enabling detailed aspects of the mechanism to be established and the rate constants to be determined; the kinetics have been interpreted within overall mechanisms that include quantitative estimates of component equilibria. These direct observations cover the whole release-and-recapture cycle and reveal subtly different kinetics and mechanisms for different cations, providing a powerful insight into the action of this generic class of photochemical switch.

Our studies have shown that the TRVIS technique can provide a useful source of information not only on excited-state cation release but also on ground-state thermal cation binding to azacrowns. In particular, it has enabled individual steps in the binding process to be observed directly in real-time, from release onward, providing a different approach to the NMR, ultrasonic absorption, or stopped-flow techniques that have often been applied. This approach may be extended to study the thermal cation binding mechanisms of other light-controlled ion switches that contain azacrowns.

In further papers, we shall report time-resolved resonance Raman and infrared spectra that provide more detailed information on the changes in structure and bonding that occur on excitation of the $ReAZBAP^+$ and $ReAZBAP^+$-M^{n+} systems.

Acknowledgment. We acknowledge financial support from EPSRC.

Supporting Information Available: Further details of steady-state UV−vis absorption and emission data on metal cation binding and time-resolved studies of $ReAZBAP^+$ in the presence of K(NCS). This material is available free of charge via the Internet at http://pubs.acs.org.

References and Notes

(1) Lehn, J.-M. *Supramolecular Chemistry*; VCH: Weinheim, Germany, 1995.
(2) *Molecular Switches*; Feringa, B. L., Ed.; Wiley-VCH: Weinheim, Germany, 2001.
(3) *Biological Applications of Photochemical Switches*; Morrison, H., Ed.; John Wiley & Sons: New York, 1993.
(4) Adams, S. R.; Kao, J. P. Y.; Grynkiewicz, G.; Minta, A.; Tsien, R. Y. *J. Am. Chem. Soc.* **1988**, *110*, 3212.
(5) Kaplan, J. H.; Ellis-Davies, G. C. R. *Proc. Natl. Acad. Sci. U.S.A.* **1988**, *85*, 6571.
(6) Adams, S. R.; Tsien, R. Y. *Annu. Rev. Physiol.* **1993**, *55*, 755.
(7) Grell, E.; Warmuth, R. *Pure Appl. Chem.* **1993**, *65*, 373.
(8) Doludda, M.; Kastenholz, F.; Lewitzki, E.; Grell, E. *J. Fluorescence* **1996**, *6*, 159.
(9) *Caged Compounds*; Marriott, G., Ed.; *Methods Enzymol., 291*; Academic Press: New York, 1998.
(10) Kimura, K.; Mizutani, R.; Yokoyama, M.; Arakawa, R.; Sakurai, Y. *J. Am. Chem. Soc.* **2000**, *122*, 5448.
(11) Shinkai, S.; Shigematsu, K.; Kusano, Y.; Manabe, O. *J. Chem. Soc., Perkin Trans. 1* **1981**, 3279.
(12) Alfimov, M. V.; Gromov, S. P.; Lednev, I. K. *Chem. Phys. Lett.* **1991**, *185*, 455.
(13) Kimura, K.; Yamashita, T.; Yokoyama, M. *J. Phys. Chem.* **1992**, *96*, 5614.
(14) Lednev, I. K.; Hester, R. E.; Moore, J. N. *J. Phys. Chem.* **1997**, *101*, 7371.
(15) Stauffer, M. T.; Knowles, D. B.; Brennan, C.; Funderburk, L.; Lin, F.-T.; Weber, S. G. *Chem. Commun.* **1997**, *3*, 287.
(16) Ushakov, E. N.; Gromov, S. P.; Buevich, A. V.; Baskin, I. I.; Fedorova, O. A.; Vedernikov, A. I.; Alfimov, M. V.; Eliasson, B.; Edlund, U. *J. Chem. Soc., Perkin Trans. 2* **1999**, 601.
(17) Gromov, S. P.; Fedorova, O. A.; Ushakov, E. N.; Buevich, A. V.; Baskin, I. I.; Parshina, Y. V.; Eliasson, B.; Edlund, U.; Alfimov, M. V. *J. Chem. Soc., Perkin Trans. 2* **1999**, 132.
(18) Alfimov, M. V.; Gromov, S. P.; Fedorov, Y. V.; Fedorova, O. A.; Vedernikov, A. I.; Churakov, A. V.; Kuz'mina, L. G.; Howard, J. A. K.; Bossmann, S.; Braun, A.; Woerner, M.; Sears, D. F., Jr.; Saltiel, J. *J. Am. Chem. Soc.* **1999**, *121*, 4992.
(19) Fedorova, O. A.; Fedorov, Y. V.; Vedernikov, A. I.; Gromov, S. P.; Yescheulova, O. V.; Alfimov, M. V.; Woerner, M.; Bossmann, S.; Braun, A,; Salteil, J. *J. Phys. Chem. A* **2002**, *106*, 6213.
(20) Malval, J.-P.; Gosse, I.; Morand, J.-P.; Lapouyade, R. *J. Am. Chem. Soc.* **2002**, *124*, 904.
(21) Alfimov, M. V.; Fedorova, O. A.; Gromov, S. P. *J. Photochem. Photobiol. A* **2003**, *158*, 183.
(22) Martin, M. M.; Plaza, P.; Dai Hung, N.; Meyer, Y. H.; Bourson, J.; Valeur, B. *Chem. Phys. Lett.* **1993**, *202*, 425.
(23) Dumon, P.; Jonusauskas, G.; Dupuy, F.; Pée, P.; Rullière, C.; Létard, J.-F.; Lapouyade, R. *J. Phys. Chem.* **1994**, *98*, 10391.
(24) Mathevet, R. M.; Jonusauskas, G.; Rullière, C.; Létard, J.-F.; Lapouyade, R. *J. Phys. Chem.* **1995**, *99*, 15709.
(25) Martin, M. M.; Plaza, P.; Meyer, Y. H.; Badaoui, F.; Lefèvre, J.-P.; Valeur, B. *J. Phys. Chem.* **1996**, *100*, 6879.
(26) Plaza, P.; Leray, I.; Changenet-Barret, P.; Martin, M. M.; Valeur, B. *Chem. Phys. Chem.* **2002**, *3*, 668.
(27) Lewis, J. D.; Moore, J. N. *Chem. Commun.* **2003**, 2858.
(28) Marcote, N.; Plaza, P.; Lavabre, D.; Fery-Forgues, S.; Martin, M. M. *J. Phys. Chem.* **2003**, *107*, 2394.
(29) Douhal, A.; Rosahl, A. D.; Organero, J. A. *Chem. Phys. Lett.* **2003**, *381*, 519.
(30) Izatt, R. M.; Pawlak, K.; Bradshaw, J. S.; Bruening, R. L. *Chem. Rev.* **1991**, *91*, 1721.
(31) Lohr, H.-G.; Vogtle, F. *Acc. Chem. Res.* **1985**, *18*, 65.
(32) Bissell, R. A.; De Silva, A. P.; Gunaratne, H. Q. N.; Lynch, P. L.; Maguire, G. E. M.; Sandanayake, K. R. A. S. *Chem. Soc. Rev.* **1992**, 187.
(33) Fabbrizzi, L.; Poggi, A. *Chem. Soc. Rev.* **1995**, 197.
(34) de Silva, A. P.; Gunaratne, H. Q. N.; Gunnlaugsson, T.; Huxley, A. J. M.; McCoy, C. P.; Rademacher, J. T.; Rice, T. E. *Chem. Rev.* **1997**, *97*, 1515.
(35) de Silva, A. P.; de Silva, S. A. *J. Chem. Soc., Chem. Commun.* **1986**, 1709.
(36) Lednev, I. K.; Hester, R. E.; Moore, J. N. *J. Chem. Soc., Faraday Trans.* **1997**, *93*, 1551.

(37) Gunnlaugsson, T.; Nieuwenhuyzen, M.; Richard, L.; Thoss, V. *J. Chem. Soc., Perkin Trans. 2* **2002**, 141.
(38) Rawle, S. C.; Moore, P.; Alcock, N. W. *J. Chem. Soc., Chem. Commun.* **1992**, 684.
(39) Anson, C. E.; Creaser, C. S.; Stephenson, G. R. *J. Chem. Soc., Chem. Commun.* **1994**, 2175.
(40) Schmittel, M.; Ammon, H. *J. Chem. Soc., Chem. Commun.* **1995**, 687.
(41) Yam, V. W.-W.; Lo, K. K.-W.; Cheung, K.-K. *Inorg. Chem.* **1995**, *34*, 4013.
(42) Yam, V. W.-W.; Lee, V. W.-M.; Ke, F.; Siu, K.-W. M. *Inorg. Chem.* **1997**, *36*, 2124.
(43) Watanabe, S.; Ikishima, S.; Matsuo, T.; Yoshida, K. *J. Am. Chem. Soc.* **2001**, *123*, 8402.
(44) Lodeiro, C.; Pina, F.; Jorge Parola, A.; Bencini, A.; Bianchi, A.; Bazzicalupi, C.; Ciattini, S.; Giorgi, C.; Masotti, A.; Valtancoli, B.; Seixas de Melo, J. *Inorg. Chem.* **2001**, *40*, 6813.
(45) Jedner, S. B.; James, R.; Perutz, R. N.; Duhme-Klair, A.-K. *J. Chem. Soc., Dalton Trans.* **2001**, 2327.
(46) MacQueen, D. B.; Schanze, K. S. *J. Am. Chem. Soc.* **1991**, *113*, 6108.
(47) Shen, Y.; Sullivan, B. P. *Inorg. Chem.* **1995**, *34*, 6235.
(48) Yam, V. W.-W.; Wong, K. M.-C.; Lee, V. W.-M.; Lo, K. K.-W.; Cheung, K.-K. *Organometallics* **1995**, *14*, 4034.
(49) Costa, I.; Fabbrizzi, L.; Pallavicini, P.; Poggi, A.; Zani, A. *Inorg. Chim. Acta* **1998**, *275*−*276*, 117.
(50) Uppadine, L. H.; Redman, J. E.; Dent, S. W.; Drew, M. G. B.; Beer, P. D. *Inorg. Chem.* **2001**, *40*, 2860.
(51) Lewis, J. D.; Moore, J. N. *Dalton Trans.* **2004**, 1376.
(52) Lewis, J. D.; Bussotti, L.; Foggi, P.; Perutz, R. N.; Moore, J. N. *J. Phys. Chem. A* **2002**, *106*, 12202.
(53) Kalyanasundaram, K. *J. Chem. Soc., Faraday Trans. 2* **1986**, *82*, 2401.
(54) Bourson, J.; Pouget, J.; Valeur, B. *J. Phys. Chem.* **1993**, *97*, 4552.
(55) Shannon, R. D. *Acta Crystallogr.* **1976**, *A32*, 751.
(56) Brzezinski, B.; Schroeder, G.; Rabold, A.; and Zundel, G. *J. Phys. Chem.* **1995**, *99*, 8519.
(57) Rurack, K.; Bricks, J. L.; Reck, G.; Radeglia, R.; Resch-Genger, U. *J. Phys. Chem. A* **2000**, *104*, 3087.
(58) The binding constants measured by UV−vis absorption studies under the conditions of our experiments (20 °C; no added electrolyte) were reproducible; they follow the same trend vs metal cation but are generally lower than those reported from emission studies of ReAZBAP$^+$−Na$^+$, −Ca^{2+}, and −Ba^{2+} in the presence of supporting electrolyte (see Table S1 in Supporting Information).[46]
(59) Fery-Forgues, S.; LeBris, M.-T.; Guetté, J. P.; Valeur, B. *J. Phys. Chem.* **1988**, *92*, 6233.
(60) Létard, J. F.; Lapouyade R.; Rettig, W. *Pure Appl. Chem.* **1993**, *65*, 1705.
(61) Rurack, K.; Sczepan, M.; Spieles, M.; Resch-Genger, U.; Rettig, W. *Chem. Phys. Lett.* **2000**, *320*, 87.
(62) Izatt, R. M.; Pawlak, K.; Bradshaw, J. S.; Bruening, R. L. *Chem. Rev.* **1995**, *95*, 2529.
(63) Schanze, K. S.; MacQueen, D. B.; Perkins, T. A.; Cabana, L. A. *Coord. Chem. Rev.* **1993**, *122*, 63.
(64) MacQueen, D. B.; Schanze, K. S. *J. Am. Chem. Soc.* **1991**, *113*, 7470.
(65) The emission lifetime and quantum yield values measured here are consistent with those reported previously, where available (see Table S1);[46] the largest difference was that the very weak emission from ReAZBAP$^+$ was measured to have a quantum yield of ca. ×2 that reported.
(66) Radiative rate constants calculated from the quantum yields and lifetimes (Table 1), using $\Phi_{em} = k_r\tau_{em}$, indicate that k_r varies with metal (4.6, 4.2, 3.4, 2.3, 1.9, and 2.0 × 10^5 for Li$^+$, Na$^+$, Mg^{2+}, Ca^{2+}, Ba^{2+}, and H$^+$, respectively). This effect was noted also by MacQueen and Schanze,[46] and our values are similar to those reported. The origin of the effect is not clear: the variation in k_r does not correlate with λ_{max}, suggesting that changes in the energy of the ILCT state are not the direct cause; nor does it correlate directly with metal cation radius, z/r ratio or binding constant. As MacQueen and Schanze noted,[46] the very weak emission[65] from ReAZBAP$^+$ may not give a reliable estimate.
(67) The short-wavelength data limit was set by the transmitted probe intensity, which varied between samples because an absorbance of ca. 0.5 at the excitation wavelength (355 nm) results in an absorbance at ca. <330 nm that depends strongly on the metal cation (Figure 1). The probe attenuation at <330 nm was strong for the Ca^{2+} and Ba^{2+} samples: the TRVIS spectra show where quantitative data were acquired, although it was evident that bleaching occurred at shorter wavelengths than those shown.
(68) The contribution of the radiative rate constant to ($k_r + k_{nr}$) is small (≲3%) for model systems such as ReBAP$^+$ or ReAZBAP$^+$-H$^+$, as obtained from the emission quantum yields and lifetimes (k_r and $k_{nr} \approx 0.2$ and 7.0 × 10^6 s^{-1}, respectively). The apparent increase in the value of k_r with metal cation[66] would be greatest for Li$^+$ and Na$^+$ ($k_r \approx 0.4 \times 10^6$ s^{-1}), but its contribution to the analysis is not significant because of a strong decrease in the lifetime of the MLCT(on) state, with k_{obs} approaching 100 × 10^7 s^{-1} in these cases due to the dominant contribution from ion release (k^*_{off}). Consequently, the value of k_r was not varied between metal cations in the kinetic analysis.
(69) Rodriguez, L. J.; Eyring, E. M.; Petrucci, S. *J. Phys. Chem.* **1989**, *93*, 5916.
(70) Eyring, E. M.; Petrucci, S.; Xu, M.; Rodriguez, L. J.; Cobranchi, D. P.; Masiker, M.; Firman, P. *Pure Appl. Chem.* **1990**, *62*, 2237.
(71) Firman, P.; Rodriguez, L. J.; Petrucci, S.; Eyring, E. M. *J. Phys. Chem.* **1992**, *96*, 2376.
(72) Firman, P.; Eyring, E. M.; Petrucci, S. *J. Phys. Chem.* **1994**, *98*, 147.
(73) Bremer, C.; Ruf, H.; Grell, E. *J. Phys. Chem. A* **1998**, *102*, 146.
(74) Buet, P.; Lewitzki, E.; Grell, E.; Albrecht-Gary, A.-M.; Wannowlus, K. J.; Mass, F.; Elias, H.; Mundt, A. A.; Dupont, Y. *Anal. Chem.* **2001**, *73*, 857.
(75) Fuoss, R. M. *J. Am. Chem. Soc.* **1958**, *80*, 5059.
(76) Kitano, H.; Hasegawa, J.; Iwai, S.; Okubo, T. *J. Phys. Chem.* **1986**, *90*, 6281.
(77) Ambundo, E. A.; Deydier, M. V.; Ochrymowycz, L. A.; Rorabacher, D. B. *Inorg. Chem.* **2000**, *39*, 1171.
(78) Pederson, C. J. *J. Am. Chem. Soc.* **1970**, *92*, 386.
(79) Eigen, M.; Tamm, K. *Z. Elektrochem.* **1962**, *66*, 93.
(80) Bernasconi, C. F. *Relaxation Kinetics*; Academic Press: New York, 1976.
(81) Loyola, V. M.; Pizer, R.; Wilkins, R. G. *J. Am. Chem. Soc.* **1977**, *99*, 7185.
(82) After a typical TRVIS experiment (≲1000 laser pulses), the absorbance at 355 nm had changed by <5%.
(83) In this estimate, diffusion coefficients of 1.03 × 10^{-5}, 1.33 × 10^{-5}, 7.9 × 10^{-6}, and 8.5 × 10^{-6} cm^2 s^{-1} were used for Li$^+$, Na$^+$, Ca^{2+}, and Ba^{2+}, respectively, in water.[84]
(84) Lide, D. R., Ed. *Handbook of Chemistry and Physics*, 1999−2000 ed.; CRC Press: London, 1999.